Electrical Railway Dynamical Versus Static Models for Infrastructure Planning and Operation

Pablo Arboleya, Clement Mayet, Alain Bouscayrol, Bassam Mohamed, Philippe Delarue, Islam El-Sayed

Electrical Railway dynamical Versus Static Models for Infrastructure Planning and Operation

Pablo Arboleya, Clément Mayet, Alain Bouscayrol, Bassam Mohamed, Philippe Delarue, Islam El-Sayed

***Abstract*—Simulation tools are essential to design the infrastructure and plan the trains operations of electrical railway systems. Traditionally, the train model (that estimates the electrical, mechanical and kinematical behaviors of the vehicles) and electrical network model (that estimates the electrical behavior of the energy supply network) are developed separately. Then, they are simulated together to estimate the interactions between both subsystems. The paper objective is to compare different models to highlight the impacts on the interactions between the vehicles and the railway electrical network, which are crucial to have accurate estimations of the system behavior. For this purpose, a new dynamical model, which is based on a systemic approach and a causality analysis, is compared to a conventional static model, which is based on a cartesian approach and a power flow analysis. The dynamical model is accurate and has been experimentally validated but requires a long computational time. The static model is fast to compute and give a good estimation of the energy consumption for conventional railway systems. However, it is not always able to estimate the power flows within the DC network, and especially when all traction power substations are blocked.**

***Index Terms*—Electrical Railways, Electrokinematical Simulation, Energetic Macroscopic Representation (EMR), Static Model, Power Flow, Modified Nodal Analysis, Non-reversible Substations, DC Traction Networks.**

I. Introduction

THE use of simulation techniques is indispensable for planning and operation electrical railways. It is indeed essential to have estimation of electrical variables such as current, voltage and power to design the infrastructure and plan the operations of electrical railway systems [1]. Since the 70's, different software and methodologies adapted to the existing vehicles and infrastructure have been proposed. The degree of complexity and the computational burden of the problems has been increased exponentially as well as the capabilities of the computers. However, the conventional approach is based on static simulations of the devices, infrastructure and vehicles, solved by means of the available power flow algorithms [2].

In DC traction networks, Traction Power Substations (TPS) play an important role in the definition problem and the selection of the solving procedure [3]. They connect the conventional AC grid with the DC traction network. Many authors proposed methods for considering both subsystems at the same time. The use of hybrid AC/DC models can be found in the literature since the decade of the 70's [4]. In addition, the braking energy management, that allows recovery of energy on the DC network during the braking phases, is another important point to consider in simulation. A direct correlation can be found between energy recovery and TPS behaviors due to interactions between the subsystems. However, these interactions are often simplified in the literature. For example, in [5], the authors provide a detailed analysis of the 12 and 24 pulses rectifiers but they do not consider regenerative braking. In [6]–[8] the authors study the impact of reversible TPS considering the energy recovery of the trains. The solving procedure is therefore simplified due to the bi-directional power flow allowed by such TPS. In [9] and [10], similar studies are provided but with wayside energy storage systems, based respectively on supercapacitors and flywheel. The work in [11] develops an integrated optimization model to obtain the speed trajectory taking into account the constraints of on-board energy storage systems (i.e. capacity, state of charge, etc.). However, no recovery energy on the network is permitted, so the braking energy can only be stored in the storage system or dissipated into the braking resistor. Similar approaches are proposed in [12] and [13], but in these cases the traction networks are not simulated and the objective is to adapt the speed profiles to minimize the net energy. Based on the same idea, the work presented in [14] optimizes the train timetable of subway systems with energy storage devices. Other interesting methodologies are presented in [15], where a combined AC/DC network is simulated with an iterative solver, and in [16], where a power flow iterative solver is proposed to consider the limitation of the network receptivity.

The simplification considering a DC equivalent of the AC network is widely accepted [9], [15]–[18]. If a proper definition of the problem is considered, nearly the same accuracy can be obtained but in a faster way [19]. This simplification allows the simulation of larger DC networks with higher number of trains. However, this can have an impact on the estimation of energetic interactions between the subsystems. Several works with different methodologies have been developed in the last decade to better consider the physical energetic interactions within DC railway systems.

The work proposed in [20] uses a power flow approach considering only the DC equivalent of the AC network. The authors put special emphasis in the description of the non-derivable and non-smooth characteristics of the trains in order to consider the effect of the overvoltage and overcurrent protections. This approach enables an accurate simulation of the overvoltage protection of the trains preventing the braking energy to be injected in the network for high catenary voltage scenarios. The methodology is able to solve meshed traction networks, but it can not consider non-reversible diode-based TPS. The authors complete the model to include non-reversible TPS in [21] by improving the solver with a modified current injection (MCI) method instead of the initial

Pablo Arboleya, Bassam Mohamed and Islam El-Sayed are with the LEMUR Research Group, Department of Electrical Engineering, University of Oviedo, Campus de Gijón, 33204, Spain

Clément Mayet is with the SATIE Laboratorie and the Conservatoire National des Arts et Métiers of Paris, France

Alain Bouscayrol and Philippe Delarue are with the L2EP of Lille, University Lille, Villeneuve d'Ascq 59655, France

Corresponding author email: arboleyapablo@uniovi.es

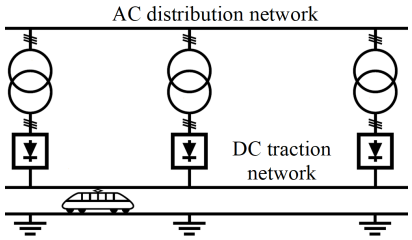

Fig. 1: Typical DC traction network

backward/forward sweep (BFS). The use of the MCI method improves the performance of the solver when dealing with meshed networks. The coupling between the train and network models is described in [22]. However, this coupling increases complexity of the system reducing the performance without adding a significant accuracy. For this reason, the coupling approach is not evolved in [23] where a complete model of the DC network is proposed with the possibility to consider controlled and non-reversible TPS, on-board and wayside energy storage systems, DC links between DC different traction networks, overcurrent and overvoltage protections, etc.

Different models (dynamical, quasi-static, static, etc.) and simulation approaches (forward and backward) for subway simulations are compared in [24] using the Energetic Macroscopic Representation (EMR) [25]. But this work is only focused on the train simulation without considering the DC network. In [26], another dynamical simulation considering both, train and DC traction network is proposed. This work takes into account the electromechanical limitations and their impact on the kinematical behavior, including overvoltage and overcurrent protections. This accurate dynamical model has been especially developed to highlight the physical interactions between the different subsystems.

This paper aims to compare the static [23] and dynamical [26] models of DC traction systems in terms of accuracy and computation time. It is the first time in the literature that such models are tested in the same traction network. This comparison should enable to decide which model to be used and for what cases. In addition, it should set the basis to construct a hybrid dynamical/static model that take advantage of the best features of each kind of models.

In section II, the general description of the system is presented considering non-reversible TPS and trains with regenerative braking. Section III presents the details of the static and dynamical models. A detailed comparative analysis of the results for both methods are carried out in section IV.

II. General Description of DC Traction Systems

A general overview of DC traction systems is provided. It is divided into power supply and train subsystems.

A. Power Supply Subsystem Description

Fig. 1 presents a typical structure of the power supply subsystem for DC railway systems. The DC traction network is connected to the AC distribution network through Traction Power Substations (TPS) consisting in a three-phase transformer and a rectifier group. The transformer converts the voltage level of the AC network to a suitable level to be used in the subsequent rectifier. The rectifier transfers the energy

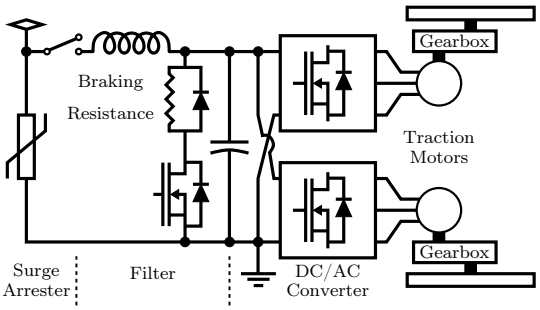

Fig. 2: Typical traction system of a DC urban train.

from the AC network to the DC network. In most of the cases, these rectifiers are based on uncontrolled diode bridges so the energy transfer is unidirectional from AC to DC.

The most typical DC voltage levels in this type of networks are 750 V, 1.5 kV and 3 kV. The transformer-rectifier group can be generally of 6 or 12 pulses. Usually, for a specific line, all TPS have a similar topology. Almost all new TPS use 12-pulse rectifiers as the induced harmonic pollution is lower. As mentioned before, the bidirectional power flow cannot be achieved with this topology. New TPS can include a Voltage Source Inverter (VSI) in parallel with the rectifier group to achieve the reversibility. The control of the VSI is generally based on the DC voltage level [8]. When it is higher than a specific threshold the converter injects power from the DC system into the AC system. This voltage threshold should be higher than the no-load voltage of the TPS. It is thus important to have accurate estimation of the DC voltage when studying such new topologies. The use of reversible TPS is not very extended even among the new infrastructures mainly for three reasons; 1) the diode-based TPS are very robust and simple; 2) traditionally, railway engineers are reluctant to change a technology that has proven to be reliable; 3) with the cost reduction of the energy storage systems, it is not clear if it is better to use reversible TPS or wayside or on-board energy storage systems to save the braking energy.

B. Train Subsystem Description

A simplified typical DC urban systems is presented in Fig. 2. The electrical connection with the feeding conductor is made through the pantograph or the third rail. A surge arrester is used to protect the train against overvoltages. The train equipments are supplied through an input filter. The braking resistance, auxiliary, and traction subsystems are connected to the DC bus. The traction subsystem can be composed of several in-wheel machines consisting in a VSI, a traction machine, a gearbox, and a wheel. Other possibility is to use the same converter to supply several traction machines.

An important aspect is related to the control and limitations of the train during the traction and braking modes. Conventional current/torque/force limitations should be respected. Additional specific limitations, such as overcurrent and overvoltage protections, must be considered because they highly impact the behavior of the train. The overcurrent protection is activated during the traction phase if the DC bus voltage V_t is too low due to high traffic, which can induce important voltage drops and high currents in the DC network. The consequence of the activation of this protection

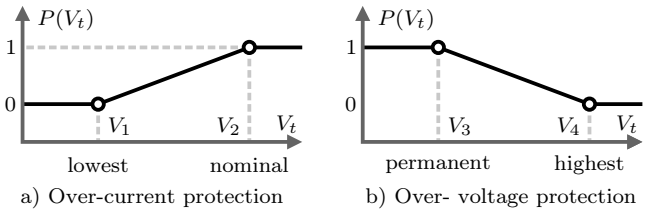

a) Over-current protection b) Over- voltage protection

Fig. 3: Overcurrent and Overvoltage protection curves

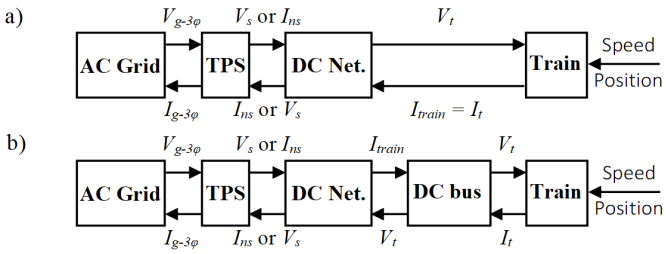

Fig. 4: Principles of a) static model, b) dynamical model

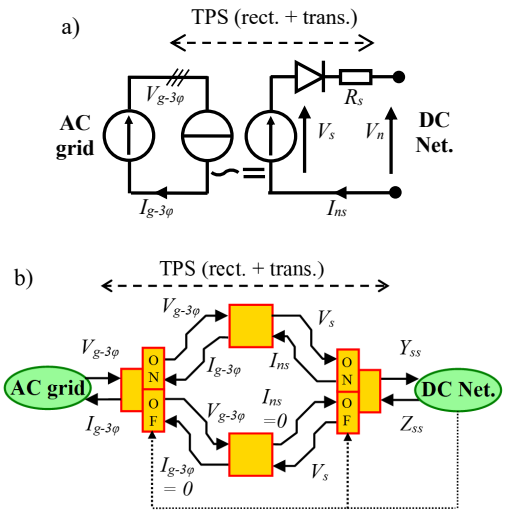

Fig. 5: TPS sub-model with the DM: a) equivalent electrical circuit, b) EMR

is to limit the available traction torque, and therefore reduce the acceleration performance. The overvoltage protection is activated during the braking phase if the voltage is too high. The reason of this voltage increasing is due to the non-reversibility of the TPS and the energy that is injected on the DC network by the different braking trains. The braking resistance must be activated in case of too high voltage for safety reasons. As a consequence, the energy recovery in braking mode is limited, and therefore the global efficiency of the system is reduced. All these limitations and protections are considered in this paper as explained in [26]. In Fig. 3, the overcurrent and overvoltage limitations of the train are represented. The traction and braking powers are respectively multiplied by the overcurrent and overvoltage protections curves depending on the DC bus voltage. As it can be observed, if the voltage is lower than V_1 the traction power will be forced to zero, the same happens with the braking power if the voltage is higher than V_4.

III. Dynamical and Static Models

This section presents two different models of the entire railway systems: dynamical (DM) and static (SM) models. The objective of such models is to accurately predict the electrical (voltage and current) and mechanical (speed and torque/force) behavior of the entire railway systems considering their non-linearity, non-reversibility and the movements of trains.

The AC grid is generally considered as main energy source, which imposes the 3-phases voltage source $V_{g-3\varphi}$ to the entire railway system (Fig. 4). Then the non-reversible TPS convert the AC variables into DC variables. They impose the DC voltage V_s to the DC network. However, due to the non-reversibility, they also impose a current I_{ns} equal to zero when their rectifiers are blocked. In conventional cartesian approach (Fig. 4.a), the train is modeled as a simple static equivalent current source I_t based on a reference power profile and the protection curves (see Fig. 3). The DC network model imposes thus the rail/catenary voltage V_t to the train, which reacts by imposing the current I_t. This generally induces simplifications on the interactions between the trains and the DC network, especially when the overvoltage protection is activated [26].

The dynamical model recently proposed is based on a systemic approach and a causality analysis [27]. The main difference with the conventional static model is to consider a dynamical model of the train DC bus to better highlight the interactions with the DC network (Fig. 4.b). With such a model, the train imposes the current I_t to the DC bus model. Then, the DC bus imposes its voltage V_t to the DC network, which reacts by imposing the current I_{train} exchanged between the DC network and the train. With this approach, the train and DC bus association is a voltage source from the DC network point of view.

These dynamical and static models are explained in the next sub-sections. The Energetic Macroscopic Representation (EMR) methodology is used as unified and common representation tool. EMR is a graphical description tool, which highlights the energy properties of complex systems and is based on the respect of the physical interactions and causality between the different components and subsystems [25].

A. Dynamical Model (DM)

The detailed dynamical model (DM) is composed of three sub-models, respectively for the TPS, the train (and DC bus), and the DC network. The TPS considers a switched-model, which has previously been developed to estimate the ON-state and OFF-state behaviors of the non-reversible TPS (Fig. 5.a) [27]. EMR is represented in Fig. 5.b. The ON-state model imposes the average rectifier open-circuit voltage V_s to the DC network (Y_{ss} = V_s) through an equivalent resistance R_s, which represents the TPS losses. It also determines the AC currents $I_{g-3\varphi}$, which are supplied by the high-voltage 3-phase grid, according to the DC current I_{ns} exchanged with the DC network (Z_{ss} = I_{ns}). The OFF-state model imposes a zero-current on the DC side (Y_{ss} = I_{ns} = 0) as well as on the AC side, and the rectifier voltage is provided (Z_{ss} = V_s). Switching conditions are defined based on the TPS characteristics and the DC network behavior [27]. The total energy consumption supplied by the AC grid can thus be estimated.

The train sub-model determines the electric power absorbed or recovered on the DC bus according to the auxiliary power and the traction subsystem power [24]. The sum of both

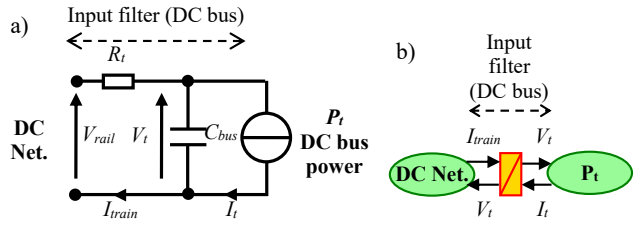

Fig. 6: Train sub-model with the DM: a) equivalent electrical circuit, b) EMR

powers is named P_{ref}. The auxiliary power is generally assumed known and can be simulated by a power profile. The traction power is estimated as a function of the velocity, the road profile (slope, wind, etc.), the losses in the different components of the electromechanical conversion and the mechanical dynamics of the train [24].

The velocity can be predetermined or can be generated by an adaptive velocity generator to adapt the electrokinematical behavior of the train according to the system limitations (overcurrent protection, torques/currents limitations, etc.) [26]. The DC bus power P_t is finally obtained by multiplying the reference power P_{ref} by the protection curves $P(V_t)$ (1) (see Fig. 3). P_t is then simulated by a voltage-dependent current source I_t (2). Moreover, one of the specificities of this dynamical model is to consider the electrical dynamics of the DC bus (Fig. 6.a). It leads to represent the vehicle (from the DC network point of view) as a variable DC voltage source V_t (3) (Fig. 6.b) with a series resistance R_t , which represent respectively the DC bus voltage and the filter losses, with V_t^{init} the initial value of the DC bus voltage, I_{train} the current exchanged between the DC bus and the catenary, C_{bus} the DC bus capacitor, and V_{rail} the catenary voltage.

$$P_t = \begin{cases} P(V_t) \cdot P_{ref} & \text{in traction mode} \\ P(V_t) \cdot P_{ref} & \text{in braking mode} \end{cases} \quad (1)$$

$$I_t = \frac{P_t}{V_t} \quad \text{DC bus current} \quad (2)$$

$$V_t = V_t^{init} + \frac{1}{C_{bus}} \int (I_{train} - I_t) dt \quad \text{DC bus voltage} \quad (3)$$

The DC network sub-model connects all the subsystems together. The mathematical model of the DC lines assumes linear resistance distribution along the line. The well-known Modified Nodal Analysis (MNA) method is used to solve the DC network [28], [29]. The MNA is generally expressed by (4), where the conductance matrix G is obtained according to the third rail or catenary resistances and the positions of the different subsystems. R is a diagonal matrix that considers the input resistances of the voltage sources (i.e. R_t for the train or R_s for the on-state TPS), and B is a matrix corresponding to the Kirchhoff currents equations [28], [29].

The subsystems (trains and TPS) impose thus the physical variables (causality) to the MNA in the input vectors J and E, respectively for the currents and voltages sources. The MNA then determines the output vectors (unknown variables) V and I, respectively the catenary voltages and the currents of the voltage sources, by inverting the MNA relationship (4). More specifically, the train model imposes the DC bus voltage V_t as input to the MNA, which determines the train current I_{train}. In the case of TPS, two states are possible for the input and output variables of the MNA (respectively Y_{ss} and Z_{ss}) as explained previously. During the ON-state, the TPS imposes its no-load rectified voltage V_s to the MNA, which reacts by imposing the TPS current I_{ns}. During the OFF-state, the TPS imposes the DC current (equal to zero) to the MNA, which determines the TPS voltage. The switches between both states are based on the physical rules described in [27].

$$\begin{bmatrix} G & -B \\ B^t & -R \end{bmatrix} \begin{bmatrix} V \\ I \end{bmatrix} = \begin{bmatrix} J \\ E \end{bmatrix} \Rightarrow \begin{bmatrix} V \\ I \end{bmatrix} = \begin{bmatrix} G & -B \\ B^t & -R \end{bmatrix}^{-1} \begin{bmatrix} J \\ E \end{bmatrix} \quad (4)$$

Algorithm 1 shows the entire solving procedure of the DM. The TPS states and DC bus voltages are used as initial conditions. Then the DC bus currents I_t are calculated by the train model based on the initial DC bus voltages, the reference power, and the protection curves; the current/voltage sources are then identified based on the TPS states (the initial states are those from the previous simulation step-time; the train are pure voltage sources); the MNA is then formulated and solved; the TPS states are then updated according to the switching conditions and MNA results; if at least one TPS state is different than its initial state a new calculation is required (GOTO 2), if not continue; finally, the trains DC bus voltages are updated for the next step time according to the currents I_t and I_{train}, which have been determined respectively from the MNA results (vector I) (step 4) and the internal train model (step 1); then end and next step-time.

Require: Init TPS states, Init DC bus voltage (V_{t-init})
1. **Update trains currents** I_t - (1) and (2)
2. **Determine current/voltage sources**
3. **Update and solve MNA** - (4)
4. **Update and save TPS states** - Switching conditions
5. **IF** TPS states chaged $\rightarrow$ **GOTO 2**
   IFNOT continue $\rightarrow$ **GOTO 6**
6. **Update DC bus voltage** - (3)
7. **END**

Algorithm 1: Simulation procedure of the DM

The respect of the physical causality imposed by the EMR leads to obtain a physical description which is perfectly able to predict the electrical and mechanical behaviors of the system. In addition, note that conventional simulation tools generally need dedicated and complex iterative numerical solvers [15]–[19]. Indeed, as simplifications on the interactions between the trains and the DC network are commonly considered with the static models, iterative methods are necessary to make solvers converge. Such methods are not necessary with this dynamical model because of the respect of the physical interactions.

An example of simple railway system composed of one TPS and two trains is represented with the EMR (Fig. 7). The EMR of the DC Network is composed of scalar/vector transformations and a matrix conversion element corresponding to the MNA relationship. This dynamical model has been validated using experimental measurements on a real system [27]. It can be used as reference in this paper.

B. Static Model (SM)

The static model (SM) is considered as the conventional steady-state model. It is based on the Modified Current

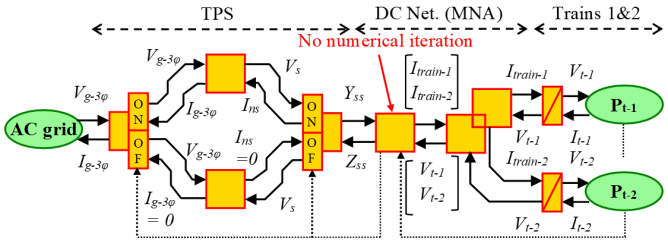

Fig. 7: EMR of the simple railway system with the DM.

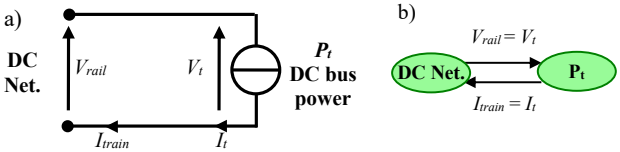

Fig. 8: Train sub-model with the SM: a) equivalent electrical circuit, b) EMR

Injection (MCI) method [21]. Each element is expressed as an equivalent current source. The general expression of the MNA (4) can therefore be simplified as (5).

$$[G]\,[V] = [J] \Rightarrow [V] = [G]^{-1}\,[J] \tag{5}$$

The DC network sub-model represents the network connections without considering the trains. A line splitting algorithm generates topology based on the positions of the trains. The lines connections are defined by the incidence matrix Γ_b where rows represent line segments and columns represent nodes. In each row, all elements are zeros except **1** at the column of the source node and **-1** at the column of the destination node as defined by:

$$\Gamma_b(row, col) = \begin{cases} 1 & col = \text{source node} \\ 0 & col = \text{others nodes} \\ -1 & col = \text{destination node} \end{cases} \tag{6}$$

The nodal conductance matrix of the lines segments G_{nb} are defined by (7), where G_b represents the conductances of the lines obtained after running the spliting procedure.

$$G_{nb} \quad = \Gamma_b^T \times G_b \times \Gamma_b \quad \text{Line conductance matrix} \tag{7}$$

The connection matrix of the trains Γ_t represents each train by a row of zeros except **1** at the column of its node:

$$\Gamma_t(row, col) = \begin{cases} 1 & col = \text{train node} \\ 0 & col = \text{other nodes} \end{cases} \tag{8}$$

The train sub-model is a constant power injection source under protection control. It provides the total DC bus power P_t but it neglects the input filter (Fig. 8). The DC bus voltage V_t is thus considered equal to the catenary voltage V_{rail} and the DC bus current I_t is considered equal to the train current I_{train}. In such model, the train is considered as a pure current source I_t. The train voltage V_t is thus calculated from the vector of nodal voltage V_n of the previous iteration using the connection matrix (9). The train current I_t is updated by (1) and (2). Then, the nodal injection current of the trains I_{nt} is defined as a summation of trains currents at each node (10).

$$V_t \quad = \Gamma_t \quad \times \quad V_n \quad \text{Train voltage} \tag{9}$$

$$I_{nt} \quad = \Gamma_t^T \quad \times \quad I_t \quad \text{Train injection current} \tag{10}$$

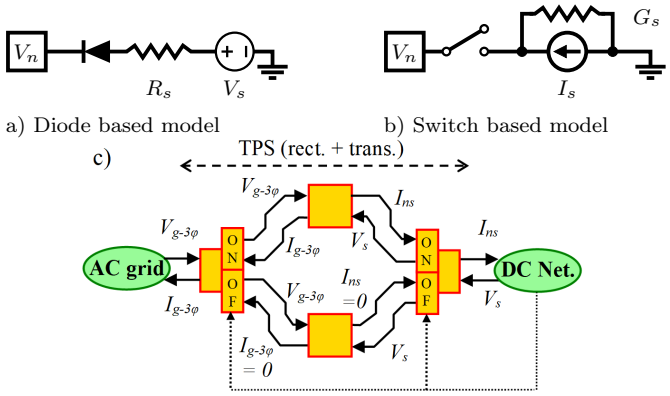

Fig. 9: TPS sub-model with the SM: a) diode-based model, b) Thevenin-Norton equivalent model, c) EMR of the Thevenin-Norton equivalent model.

The TPS submodel uses a Thevenin-Norton equivalent circuit. Fig. 9.a shows a non-reversible substation model based on an ideal diode in a series with slack resistance R_s and slack voltage source V_s (idem to Fig. 5.a). Fig 9.b simplifies the model by a switch connected to a Thevenin-Norton equivalent circuit with a slack conductance ($G_s = R_s^{-1}$) and a slack current source ($I_s = G_s \times V_s$). Fig. 9.c) is the equivalent EMR. The mathematical model of the TPS is therefore defined by a current injection I_{ns} and shunt conductance G_{ns} based on the TPS state (ON/OFF) (11). The nodal conductance matrix G_n and the nodal injection current I_n are then updated by (12).

$$\begin{array}{ll} \text{OFF} & V_n \geqslant V_s \Rightarrow I_{ns} = 0 \quad , \; G_{ns} = 0 \\ \text{ON} & V_n < V_s \Rightarrow I_{ns} = -G_s \times V_s \quad , \; G_{ns} = G_s \end{array} \tag{11}$$

$$I_n = I_{nt} + I_{ns} \quad , \quad G_n = G_{nb} + G_{ns} \tag{12}$$

Algorithm 2 shows the steps implemented for solving this model. As all elements are modeled as equivalent current sources, the objective of Algorithm 2 is to determine each voltage node. A dedicated iterative numerical solver is needed because switching devices models use non-smooth functions with discontinuities in their derivatives, which may introduce oscillation or diversion for conventional solvers. Initially, all nodal voltages are set to one and all nodal injection currents to zero. First, the old values of the nodal voltages and currents are saved. Then, the MNA is updated based on the models of trains and TPS and is solved to get the new nodal voltage V_n^{new}. An intermediate point is then selected between old and new voltage using the damping factor α to avoid convergence problems (13). Low values of α reduce the solver speed while higher values may cause a diversion. The solver error (err) is defined based on the norm difference between iterations in nodal voltages and currents (14). The iterative solver stops when the error becomes lower than the tolerance.

$$V_n = V_n^{old} + \alpha \cdot (V_n^{new} - V_n^{old}) \qquad 0.01 < \alpha < 1 \tag{13}$$

$$err = \|I_n - I_n^{old}\| + \|V_n^{new} - V_n^{old}\| \tag{14}$$

This static model is also described using EMR (Fig. 10). The difference is that the DC bus is now not considered (see Fig. 7). Inputs and outputs of the MNA are therefore not the same, so a dedicated numerical iterative solver is now needed because the causality is no longer respected.

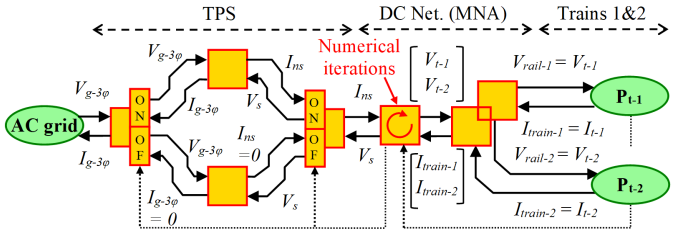

Fig. 10: EMR of the simple railway system with the SM.

IV. Comparative Analysis of the Results

A. Description of the Scenario

A specific scenario has been defined in order to compare the different models. For this purpose, a 6.8 km conventional light rail system composed of 7 passenger stations (PS) and supplied by 3 conventional TPS is considered (Fig. 11). This test line is derived from the subway line B of the city of Rennes in France (data have been changed for confidentiality reasons). All TPS are supposed identical. The main characteristics of the power supply subsystem are summarized in Table I [26]. A light automatic subway is considered. It is composed of 2 cars, and each car have 4 in-wheel electric drives [24]. The headway considered in this study is 120s, which requires 10 trains on the studied line. Furthermore, it is assumed that there is no traffic at the beginning of the simulation. The different trains (T1 to T10) are thus injected on the line from PS1 and PS7 as presented on Fig. 12. The velocity profiles have been defined to respect the electrokinematical limitations [26]. The DM, which has been previously validated by comparison with experimental measurements on real DC traction system [27], is used as reference for comparisons with the SM.

B. Results and Comparisons

The results obtained from the simulations are presented in Figs. 13 and 14 and Tables II, III and IV. The figures contain temporal variation of the electrical variables like power, accumulated energy, voltage and current, while the tables present the total energy transferred, provided or consumed in different subsystems of the network. In the DM, the input filter of the train is modeled in a detailed way considering the filter efficiency. In the SM, the reference power (P_{ref}) has been adapted considering an equivalent efficiency of the input filter. It can be noted that in most existing simulation tools, the input filter is not simulated and its losses are neglected.

Require: $V_s, R_s, P_{ref}, \alpha$, **Output:** V_n

1. **Initialize variables** $V_n = 1$, $I_n = 0$
2. **Save old variables** $V_n^{old} = V_n$, $I_n^{old} = I_n$
3. **Update train current** - (2) and (10)
4. **Update substation state** - (11)
5. **Update MNA** $I_n = I_{nt} + I_{ns}$, $G_n = G_{nb} + G_{ns}$
6. **Solve** $G_n \times V_n^{new} + I_n = 0$
7. **Damping** $V_n = V_n^{old} + \alpha \cdot (V_n^{new} - V_n^{old})$
8. **Get error** $err = \|I_n - I_n^{old}\| + \|V_n^{new} - V_n^{old}\|$
9. **IF** $err > \epsilon$ **GOTO** 2
10. **END**

Algorithm 2: Simulation procedure of the SM

TABLE I: Characteristics of the power supply subsystem

Positions of the TPS (m)	x_1, x_2, x_3	0, 3580, 6862
Phase to phase grid voltage (AC) (kV)	U_{res}	20
No-load TPS rectified voltage (DC) (V)	E_{ss}	750.8
TPS losses equivalent resistance ($m\Omega$)	R_{ss}	23.1
Rail resistance per meter ($\mu\Omega/m$)	R_{lin}	26

TABLE II: Energetic analysis for DM and SM.

DM results	TPS1	TPS2	TPS3	All TPSs
Energy in AC side (kWh)	109,1	165,6	88,1	362,8
Energy in DC side (kWh)	106,3	159,8	86,4	352,5
Losses (kWh)	2,8	5,8	1,7	10,3
Losses (%) respect AC	2,6	3,5	2,0	2,8
SM results	**TPS1**	**TPS2**	**TPS3**	**All TPSs**
Energy in AC side (kWh)	108,8	165,7	87,5	362,0
Energy in DC side (kWh)	105,7	159,1	85,8	350,6
Losses (kWh)	3,0	6,6	1,8	11,4
Losses (%) respect AC	2,8	4,0	2,0	3,1

In Table II, the energy provided by all TPS are analyzed. The table contains information about the losses in (kWh) and the losses in (%) respect to the energy provided from the AC side. The values obtained with the DM and SM simulations are very similar with an error in the total energy provided by the AC side of 0.2%. It must be remarked that the energy sharing among the 3 TPS is also very similar.

The detailed behavior of the train 1 (T1) during the whole simulation (left part of Fig. 13) and a zoomed analysis between 450 s and 550 s (right part of Fig. 13) are provided. The signals depicted are the power reference P_{ref} (without the filter losses) (Fig. 13a), the net energy of T1 at the catenary side (Fig. 13b), the mismatch power between P_{ref} and the actual power exchanged with the catenary (Fig. 13c), the catenary voltage (Fig. 13d) and the current exchanged between T1 and the catenary (Fig. 13e). The DM and the SM provide globally equivalent results. However, at some instants, the differences

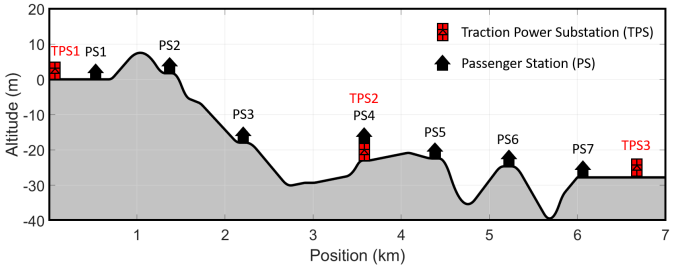

Fig. 11: Profile of the studied line.

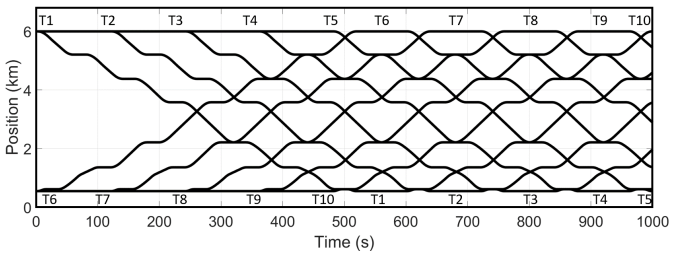

Fig. 12: Circulation mesh of the studied case.

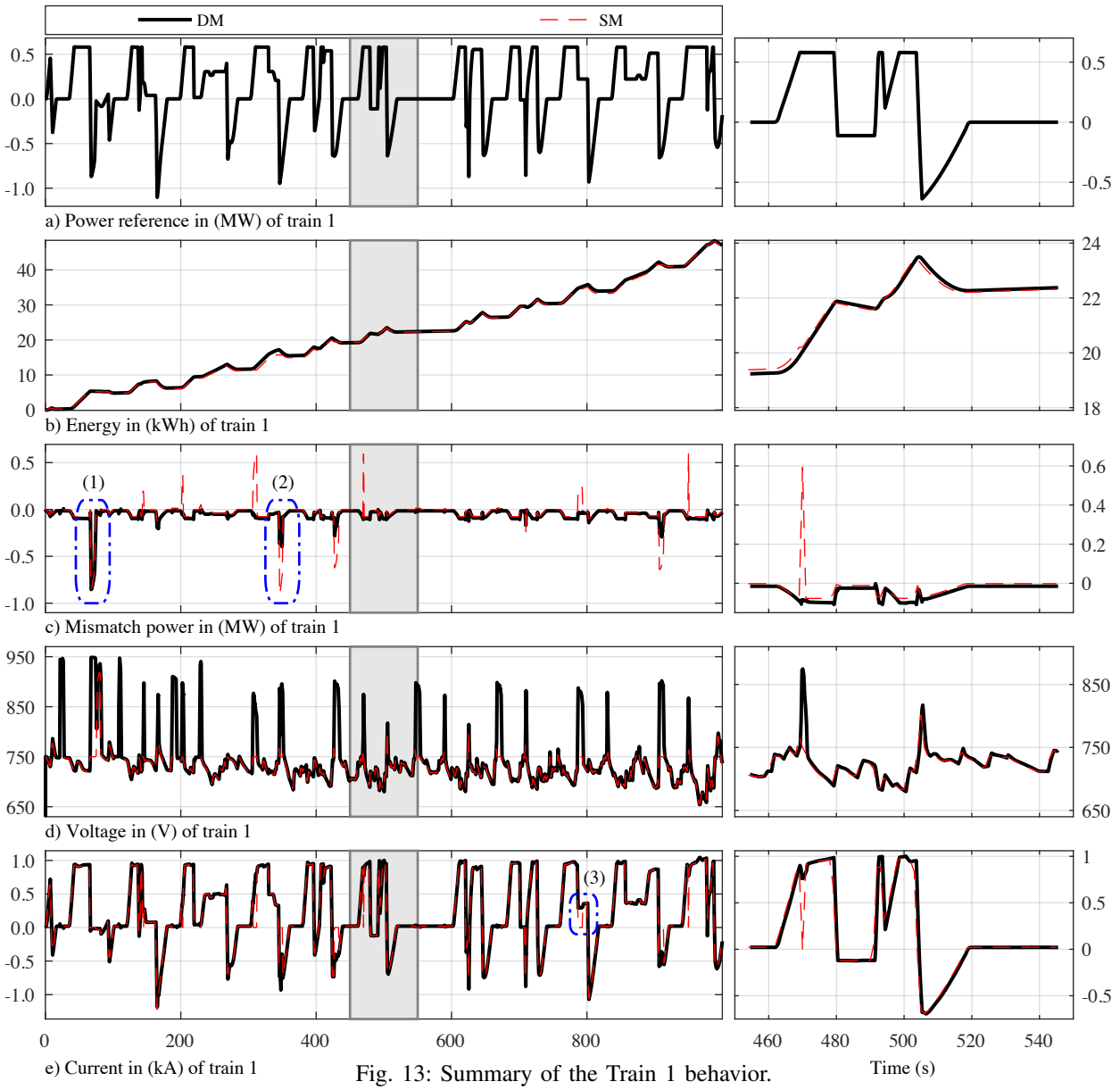

Fig. 13: Summary of the Train 1 behavior.

are important. For instance, 3 points have been highlighted in Fig. 13 to analyze these differences. Fig. 14 highlights these differences considering the studied train (T1), an equivalent TPS (TPS_{eq}) representing all the TPS, and an equivalent train (T_{eq}) representing all the other trains (T2 to T10). Note that the equivalent TPS is blocked for all the highlighted points, which means all TPS are blocked at the same time.

Point 1 highlights an important power mismatch for both models between the reference power and the actual negative power (around 0.8 MW). Indeed, the train regenerates 0.8 MW but all power is dissipated in the braking resistance. The train current is thus zero due to the activation of the overvoltage protection with the DM and the SM. However, the SM returns the rated voltage (750 V) instead of the maximal voltage (950 V). Point 2 is quite different, the power mismatch is 0.8 MW with the SM but only 0.4 MW with the DM. It means that with the DM the train injects on the catenary around 0.4 MW of the 0.8 MW braking power, the rest is dissipated into the brake. With the SM, all the braking power is dissipated into the brake. Furthermore, the DM can provide the correct value of the catenary voltage and current with respectively 870 V and -460 A, whereas they are 750 V and 0 A with the SM. In the point 3, the train has a moderate consumption of around 250 kW. The power mismatch with the DM simulation is very small and corresponds to the input filter losses. With the SM, the mismatch is positive and equal to the reference power, which means that the train consumes no power. Indeed, even when T1 consumes power, the total amount of power recovered in the system leads to block all TPS and SM algorithms provide the trivial solution (rated voltage and zero current). As it can be observed, whenever this issue occurs, the voltage with the DM simulation is very high.

It can thus be stated that the source of the mismatch between DM and SM is the inability of the existing SM to solve the DC network when it is isolated from the AC grid. The DM simulation is completely accurate in these cases, whereas the SM provides the trivial solution: all voltages equal to the rated voltage and all currents and powers equal to zero. It does

TABLE III: Energetic analysis of all the trains in the system for DM and SM.

DM results	Train 1	Train 2	Train 3	Train 4	Train 5	Train 6	Train 7	Train 8	Train 9	Train 10	All Trains
Absorbed Energy (kWh)	64.2	53.4	43.1	36.7	31.7	62.2	54.2	47.4	39.1	37.8	469.7
Energy Recovered (kWh)	17.0	15.3	13.7	10.8	10.4	16.7	14.8	11.8	10.4	10.0	130.9
Net Energy (kWh)	47.1	38.1	29.4	25.9	21.3	45.6	39.4	35.6	28.7	27.8	338.8
SM results	**Train 1**	**Train 2**	**Train 3**	**Train 4**	**Train 5**	**Train 6**	**Train 7**	**Train 8**	**Train 9**	**Train 10**	**All Trains**
Absorbed Energy (kWh)	61.5	51.2	41.4	35.2	30.1	58.7	52.5	45.8	37.7	36.3	450.5
Recovered Energy (kWh)	14,5	13,6	11,9	9.0	8.6	14.5	12.8	9.7	9.2	8.9	112.8
Net Energy (kWh)	47.0	37.6	29.5	26.2	21.5	44.3	39.7	36.1	28.4	27.4	337.7

TABLE IV: Summary of all energies consumed in the system and the overall errors for DM and SM.

	Substations			Trains			Grid
	AC side	DC side	Losses	Absorbed	Recovered	Net	Losses
Energy with DM (kWh)	362.8	352.5	10.3	469.7	130.9	338.8	13.6
Energy with SM (kWh)	362.0	350.6	11.4	450.5	112.8	337.7	12.9
Error with SM (%)	-0.2	-0.5	10.3	-4.1	-13.8	-0.3	-5.1

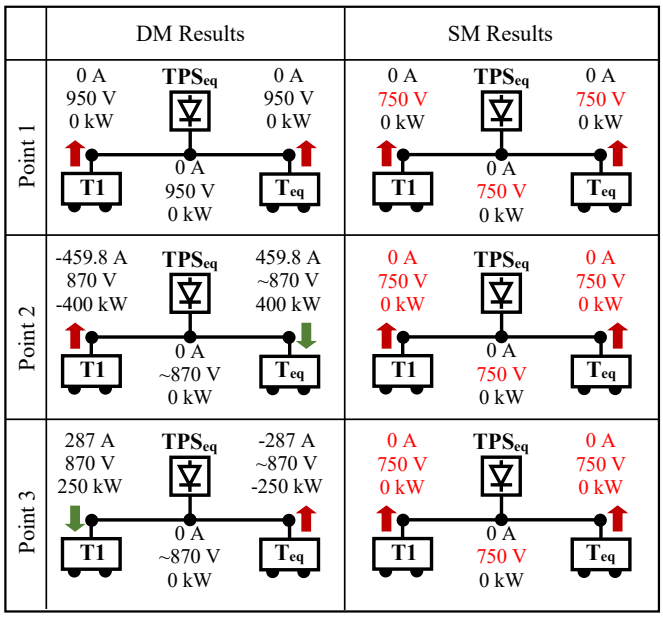

Fig. 14: Differences highlighted on the 3 studied points.

not affect the power provided by the TPS because they only happen when all TPS are blocked, (in this case around 10% of the time), but they affect the power flow within the DC network and the voltage estimation.

Table III presents an energetic analysis of all trains with both simulations. It summarizes the total absorbed, recovered, and net energy. The SM always provides lower values of absorbed and regenerated energy compared to the DM. The errors on the absorbed energy with the SM are between 3.1 % and 5.6 %, with a total error of 4.1 % for all trains. The errors are more important on the recovered energy, between 11 % and 17.8 %, with a total error of 13.8 % for all trains. Finally, the errors on the net energy are between 2.9 % to -1.4 %, with an average error of 0.3 % for all trains. In addition, Table IV summarizes the energies in the TPS and the trains, as well as the losses estimations of the DC network. The DM estimates a total loss in the DC network of 13.6 kWh. The error with the SM is -5.1 %. Obviously these losses will be always higher with the DM because the power flows within the DC network are neglected with the SM when all TPS are blocked.

C. Discussion

In order to obtain a useful simulation tool for the design process of the entire system, considering the feeding infrastructure and the vehicles, three items are particularly of importance: the accuracy of the simulation model, the computation time (to optimize the system with high number of scenarios) and the availability of the model parameters.

Regarding the results accuracy, the DM is perfectly able to simulate the entire system in all the studied cases, whereas the SM is not able to provide the correct solution when all TPS are blocked. More particularly the DM allows a better estimation of the power flow and voltage evolution in the DC network during the braking phases, which is clearly of importance to study innovative supply structures with energy storage system (ESS) or reversible TPS. Indeed, the use of such sub-systems is mainly determined based on the DC network voltage because of their common considered controls. It is therefore during these instants that such innovative systems are particularly of interest to store the braking energy. A comparative study between DM and SM with innovative sub-systems would be necessary to quantify the errors in the sizing of such sub-systems or in the energy saving estimation.

Regarding the computation time, the SM is clearly fastest than the DM. Indeed, the time invested by the SM for solving the whole simulation interval of 1000s is lower than 3.5s while the DM invests approximately 736s. It is due to the small step time required by the DM to compute the small dynamics of the input filter (DC bus), which is not required with the SM.

Another important aspect is the availability of the model parameters. The SM requires only the reference power profile and the equivalent efficiency for the train sub-model. Note that the adjustment of this equivalent efficiency can have a strong impact on the results accuracy. It has been demonstrated that with the proper tuning, the SM can provide equivalent results than the DM in terms of global power and energy consumption of the railway system. The error in the total energy estimation provided by the TPS with the SM can be neglected but the

train efficiency must be perfectly adjusted to consider all the components losses, including the input filter. In the other side, the DM does not require equivalent efficiency but needs specific additional parameters such as the input capacitor and the resistance of the filter inductor for example.

V. Conclusions

Simulation of the railway feeding infrastructure together with the vehicles is a critical issue for the correct sizing and operation of such systems. There are two trends for making this kind of simulations: static model and dynamical model. These models have been briefly presented in this paper, and for the first time in the literature, have been applied and compared on the same studied system. The comparisons highlight that the static model cannot provide the solution when the traction system is completely disconnected from the AC slack (all traction power substations are blocked), which can happen more or less frequently depending on the studied system. In such a case, it returns the trivial solution (voltages at one p.u. and zero currents). The dynamical model can handle this situation without problem and estimate the power flows and voltages within the DC network in all cases. This last point is crucial for studying innovative technologies aimed at saving braking energy. However, in terms of computation time, the static model is much faster than the dynamical model. Note also that, with the static model, the tuning of the global equivalent efficiency of the train sub-model is very sensitive and can have huge impact on the results accuracy.

With the conclusions of this work, it is possible to draw a guideline to select the right model to use according to the objective of the study. For example, the static model is suitable for estimating the global energy consumption, sizing traction power substations, and selecting the main topology of railway systems. It can also be considered for optimization purposes. However, it is less efficient for estimating, locally and accurately, the power flows and the evolution of the voltage level within the DC network. The dynamical model can perfectly achieve such estimations and can be used to study several local controls of different types of subsystems and their sizing. But it can not be used for optimization purposes due to its high computation load. Finally, it would be interesting to take the advantage of the benefits of both methods, the speed of the static method combined with the accuracy of the dynamical model. As a future work, the authors propose the implementation of hybrid methodologies to exploit the best features of both approaches.

Acknowledgment

The authors would like to thank to CAF Turnkey & Engineering, specially to Peru Bidaguren and Urtzi Armendariz for their support during the development of the research for developing the static simulators.

References

[1] R. Barrero, J. V. Mierlo, and X. Tackoen, "Energy savings in public transport," *IEEE Vehicular Technology Magazine*, vol. 3, no. 3, pp. 26–36, Sep. 2008.

[2] M. Khodaparastan, A. A. Mohamed, and W. Brandauer, "Recuperation of regenerative braking energy in electric rail transit systems," *IEEE Transactions on Intelligent Transportation Systems*, vol. 20, no. 8, pp. 2831–2847, Aug 2019.

[3] M. Chymera and C. J. Goodman, "Overview of electric railway systems and the calculation of train performance," in *IET Professional Development Course on Electric Traction Systems (2012)*, Nov 2012, pp. 1–18.

[4] D. Braunagel, L. Kraft, and J. Whysong, "Inclusion of DC converter and transmission equations directly in a Newton power flow," *Power Apparatus and Systems, IEEE Transactions on*, vol. 95, no. 1, pp. 76–88, 1976.

[5] Y. Tzeng, R. Wu, and N. Chen, "A detailed R-L fed bridge converter model for power flow studies in industrial AC/DC power systems," *Industrial Electronics, IEEE Transactions on*, vol. 42, no. 5, pp. 531–538, 1995.

[6] T. Suzuki, "DC power-supply system with inverting substations for traction systems using regenerative brakes," *Electric Power Applications, IEE Proceedings B*, vol. 129, no. 1, pp. 18 –26, january 1982.

[7] Y. Tzeng, R. Wu, and N. Chen, "Electric network solutions of DC transit systems with inverting substations," *Vehicular Technology, IEEE Transactions on*, vol. 47, no. 4, pp. 1405–1412, 1998.

[8] G. Zhang, Z. Tian, P. Tricoli, S. Hillmansen, Y. Wang, and Z. Liu, "Inverter operating characteristics optimization for dc traction power supply systems," *IEEE Transactions on Vehicular Technology*, vol. 68, no. 4, pp. 3400–3410, April 2019.

[9] A. M. Gee and R. W. Dunn, "Analysis of trackside flywheel energy storage in light rail systems," *IEEE Transactions on Vehicular Technology*, vol. 64, no. 9, pp. 3858–3869, Sep. 2015.

[10] Z. Yang, Z. Yang, H. Xia, and F. Lin, "Brake voltage following control of supercapacitor-based energy storage systems in metro considering train operation state," *IEEE Transactions on Industrial Electronics*, vol. 65, no. 8, pp. 6751–6761, Aug 2018.

[11] C. Wu, W. Zhang, S. Lu, Z. Tan, F. Xue, and J. Yang, "Train speed trajectory optimization with on-board energy storage device," *IEEE Transactions on Intelligent Transportation Systems*, vol. 20, no. 11, pp. 4092–4102, Nov 2019.

[12] Z. Hou, H. Dong, S. Gao, G. Nicholson, L. Chen, and C. Roberts, "Energy-saving metro train timetable rescheduling model considering ato profiles and dynamic passenger flow," *IEEE Transactions on Intelligent Transportation Systems*, vol. 20, no. 7, pp. 2774–2785, July 2019.

[13] J. Feng, Z. Ye, C. Wang, M. Xu, and S. Labi, "An integrated optimization model for energy saving in metro operations," *IEEE Transactions on Intelligent Transportation Systems*, vol. 20, no. 8, pp. 3059–3069, Aug 2019.

[14] P. Liu, L. Yang, Z. Gao, Y. Huang, S. Li, and Y. Gao, "Energy-efficient train timetable optimization in the subway system with energy storage devices," *IEEE Transactions on Intelligent Transportation Systems*, vol. 19, no. 12, pp. 3947–3963, Dec 2018.

[15] T. Ho, Y. Chi, L. Siu, and L. Ferreira, "Traction power system simulation in electrified railways," *Journal of Transportation Systems Engineering and Information Technology*, vol. 5, no. 3, pp. 93–107, 2005.

[16] R. A. Jabr and I. Džafić, "Solution of dc railway traction power flow systems including limited network receptivity," *IEEE Transactions on Power Systems*, vol. 33, no. 1, pp. 962–969, Jan 2018.

[17] C. Pires, S. Nabeta, and J. Cardoso, "ICCG method applied to solve dc traction load flow including earthing models," *Electric Power Applications, IET*, vol. 1, no. 2, pp. 193–198, March 2007.

[18] Y. Cai, M. Irving, and S. Case, "Modelling and numerical solution of multibranched DC rail traction power systems," *Electric Power Applications, IEE Proceedings -*, vol. 142, no. 5, pp. 323–328, Sep 1995.

[19] ——, "Iterative techniques for the solution of complex DC-rail-traction systems including regenerative braking," *Generation, Transmission and Distribution, IEE Proceedings-*, vol. 142, no. 5, pp. 445–452, Sep 1995.

[20] P. Arboleya, B. Mohamed, C. González-Morán, and I. El-Sayed, "BFS algorithm for voltage-constrained meshed DC traction networks with nonsmooth voltage-dependent loads and generators," *IEEE Transactions on Power Systems*, vol. 31, no. 2, pp. 1526–1536, March 2016.

[21] B. Mohamed, P. Arboleya, and C. González-Morán, "Modified current injection method for power flow analysis in heavy-meshed DC

railway networks with nonreversible substations," *IEEE Transactions on Vehicular Technology*, vol. 66, no. 9, pp. 7688–7696, Sept 2017.

[22] P. Arboleya, "Heterogeneous multiscale method for multirate railway traction systems analysis," *IEEE Transactions on Intelligent Transportation Systems*, vol. 18, no. 9, pp. 2575–2580, Sept 2017.

[23] P. Arboleya, B. Mohamed, and I. El-Sayed, "DC railway simulation including controllable power electronic and energy storage devices," *IEEE Transactions on Power Systems*, vol. 33, no. 5, pp. 5319–5329, Sept 2018.

[24] C. Mayet, L. Horrein, A. Bouscayrol, P. Delarue, J. N. Verhille, E. Chattot, and B. Lemaire-Semail, "Comparison of different models and simulation approaches for the energetic study of a subway," *IEEE Transactions on Vehicular Technology*, vol. 63, no. 2, pp. 556–565, Feb 2014.

[25] A. Bouscayrol, J.-P. Hautier, and B. Lemaire-Semail, *Graphic formalism for the control of multi-physical energetic systems: COG and EMR in Systemic Design Methodologies for Electrical Energy System*. NJ, USA: Hoboken, Wiley, 2012.

[26] C. Mayet, A. Bouscayrol, P. Delarue, E. Chattot, and J. N. Verhille, "Electrokinematical simulation for flexible energetic studies of railway systems," *IEEE Transactions on Industrial Electronics*, vol. 65, no. 4, pp. 3592–3600, April 2018.

[27] C. Mayet, P. Delarue, A. Bouscayrol, E. Chattot, and J. N. Verhille, "Comparison of different EMR-based models of traction power substations for energetic studies of subway lines," *IEEE Transactions on Vehicular Technology*, vol. 65, no. 3, pp. 1021–1029, Mar 2016.

[28] C.-W. Ho, A. Ruehli, and P. Brennan, "The modified nodal approach to network analysis," *IEEE Transactions on Circuits and Systems*, vol. 22, no. 6, pp. 504–509, June 1975.

[29] V. Acary, O. Bonnefon, and B. Brogliato, *Nonsmooth modelling and simulation for switched circuits*. Springer Science & Business Media, 2010.

Pablo Arboleya (SM'13) received the M.Sc. and Ph.D. (with distinction) degrees from the University of Oviedo, Gijón, Spain, in 2001 and 2005, respectively, both in Electrical Engineering. Nowadays, he works as Associate Professor in the Department of Electrical Engineering at the University of Oviedo, he is Managing Editor of the International Journal of Electrical Power and Energy Systems and holder of the Gijón Smart Cities Chair at the University of Oviedo. Presently his main research interests are focused in the micro-grid and smart-grid modeling and operation techniques, Internet of the Energy applications, railway traction networks simulation and combined AC/DC power flow algorithms.

Clément Mayet (M'20) received his Ph.D. degree in Electrical Engineering in 2016 from the University of Lille, France. Then, he held a post-doctoral position at the University of Lille and the L2EP. From 2017 to 2018, he was senior researcher at the MOBI research group at the Vrije Universiteit of Brussels, Belgium. Since September 2018 he is Associate Professor at the Conservatoire National des Arts et Métiers of Paris, France, and the SATIE laboratory. His research interests include graphical descriptions, modelling, control, energy management, and hardware-in-the-loop simulation of Electric and Hybrid Vehicles, including railway system.

Alain Bouscayrol (M'02) received the Ph.D. degree from the Institut National Polytechnique de Toulouse, Toulouse, France, in 1995. From 1996 to 2005, he was an Associate Professor with University Lille1, France, where he has been a Professor since 2005. Since 2004, he has managed the French national network on energy management of HEV. He has initiated the Energetic Macroscopic Representation in 2000. His research interests include graphical descriptions for control of wind energy conversion systems, railway traction systems, hybrid vehicles, and HIL simulation.

Bassam Mohamed received the M.Sc and Ph.D. degrees from the University of Oviedo, Gijón, Spain, in 2014 and 2018 respectively. He is now responsible of railway software development at LEMUR Research Group. His field of expertise has to do with the efficient design and implementation of algorithms for power systems analysis, specially those related to railway networks and unbalanced micro-grids. During the last years he developed several commercial software packages for electric network analysis and simulation.

Philippe Delarue received the Ph.D. degree from the University Lille1, Villeneuve d'Ascq, France, in 1989. Since 1991, he has been an Assistant Professor with Polytech'Lille, Villeneuve d'Ascq, France. He is currently with the L2EP of Lille, University Lille1. His main research interests include power electronics and multimachines systems.

Islam El-Sayed was born in Zagazig, Egypt, in 1984. He received the B.Sc. degree in electrical engineering from Zagazig University, Zagazig, Egypt, in 2006, and the Ph.D. degree from the Department of Electrical, Computer, and Systems Engineering, University of Oviedo, Gijón, Spain, in 2012. His ongoing research is connected with the application of big data, visual analytics to power systems analysis. Islam works also in the development of techniques to allow the massive penetration of new technologies like Internet of the Things in Low Voltage distribution systems.